

Models of the ox1 State of Methylcoenzyme M Reductase: Where are the Electrons?

Emmanuel Gonzalez and Abhik Ghosh*^[a]

Abstract: The nature of the nickel center in the ox1 form of methylcoenzyme M reductase (MCR_{ox1}), the enzyme that catalyzes the last step of biological methanogenesis, has long been controversial. A recent pulse electron paramagnetic resonance (EPR) study suggested a Ni^{III}-thiolate, or equivalently a high-spin Ni^{II} thiyl radical, description. The MCR_{ox1} hyperfine parameters are best interpreted in terms of a Ni d_{x²-y²} SOMO, although a pure d_{x²-y²} SOMO does not explain the fact that about 7% of the spin-density resides on the sulfur. The key goals of this DFT (PW91) study were to judge whether the Ni^{III}-thiolate description is chemically sensible and, if so, to provide a detailed molecular orbital (MO) description of MCR_{ox1}. An Ni^{III}-thio-

late description was indeed found to be reasonable and was obtained as the ground state for symmetrized (C_s) oxaporphyrin-, pyriporphyrin-, and isoporphyrin-based model complexes, as well as for a more realistic, biomimetic model. The model calculations yielded a number of insights, key among which are the following: 1) Although the SOMO topology may be viewed as d_{x²-y²}-like, this MO also has a substantial amount of metal d_{z²} character, allowing it to overlap with a thiolate σ lone pair, which would otherwise be orthogonal. 2) In one case (isoporphyrin),

Keywords: density functional calculations • electronic structure • enzymes • EPR spectroscopy • nickel

we were able to exploit the symmetry of the molecule to independently optimize the (d_{x²-y²})¹ and (d_{z²})¹ Ni^{III} states, which turned out to be very close in energy. 3) The near-degeneracy of these two states provides an elegant explanation for the tendency of these two orbitals to hybridize. Admixture of substantial d_{z²} character into the d_{x²-y²}-type SOMO of our most realistic model of MCR_{ox1} results in a small but distinct spin population of about 0.04 on the sulfur, apparently nicely confirming the conclusions derived from the pulse EPR study. Other pure functionals also confirm this picture, although the hybrid functional B3LYP yields a spin-density profile that is clearly at odds with the EPR study.

Introduction

The methanogens are a class of the strictly anaerobic Archaea that derive their energy by the stepwise reduction of carbon dioxide to methane (the methanogenesis cycle).^[1] The elucidation of the biochemical pathway of methanogenesis, largely by the research groups of Wolfe^[2] and Tauer,^[3] over the past quarter-century, stands as a landmark in biochemistry. In the course of the methanogenesis process, a one-carbon fragment is passed between a number of unusual cofactors. Our focus here is on the last, methane-evolving


step of this process, which consists of the two-electron reduction of a methylthioether, coenzyme M (CH₃-S-CoM), by a thiol, coenzyme B (N-7-mercaptoheptanoylthreonine phosphate, CoB-SH), as shown in Equation (1):



The reaction is catalyzed by the enzyme methylcoenzyme M reductase (MCR).^[4] A key component of the active site of MCR is coenzyme F₄₃₀,^[4] a unique and highly reduced nickel hydroporphyrin, whose structure is shown in Figure 1. The active form of the enzyme, referred to as MCR_{red1}, features the (presumably) tetracoordinate d_{x²-y²}¹ nickel(I) state of the cofactor,^[4] whose stability is due primarily to the mono-anionic nature of the F₄₃₀ ligand (as distinguished from dianionic porphyrin ligands). Several additional forms of the enzyme are known.

In this study, we are concerned with an enzymatically inactive but “ready” form of the enzyme, MCR_{ox1}, which can

[a] Dr. E. Gonzalez, Prof. Dr. A. Ghosh
Department of Chemistry and
Center for Theoretical and Experimental Chemistry
University of Tromsø, 9037 Tromsø (Norway)
Fax: (+47) 7764-4765
E-mail: abhik@chem.uit.no

 Supporting information for this article is available on the WWW under <http://dx.doi.org/10.1002/chem.200800648>. It contains optimized ground-state coordinates for the various species studied.

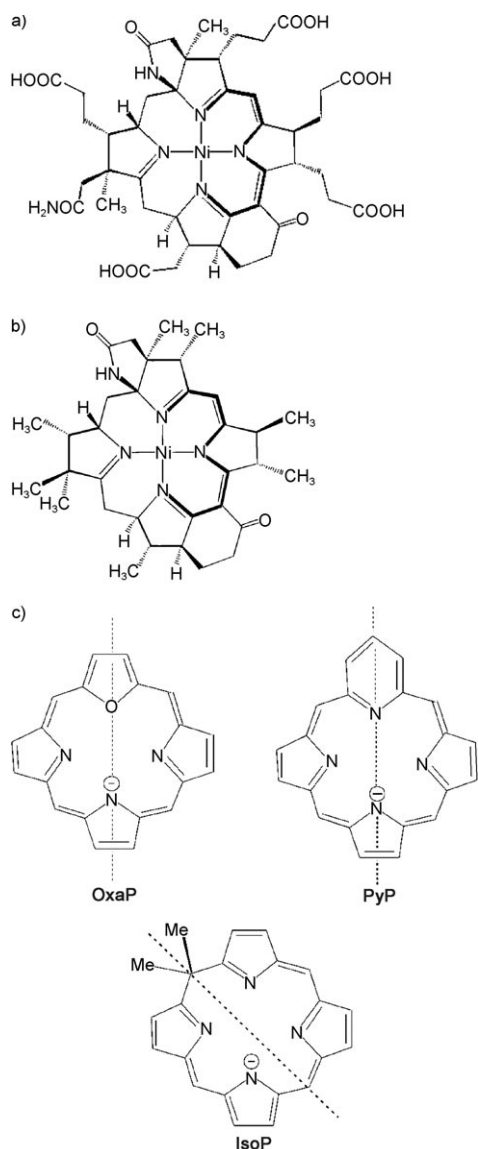


Figure 1. Structures of interest: a) coenzyme F_{430} , b) our simplified model F'_{430} , and c) model ligands used in this study, including oxaporphyrin (OxaP), pyriporphyrin (PyP), and dimethylisoporphyrin (IsoP).

be readily reduced to the active red1 state. The MCR_{ox1} form is to be distinguished from $MCR_{ox1-silent}$, an electron paramagnetic resonance (EPR)-silent $S=1$ Ni^{II} state, that cannot be readily reduced to red1. A crystal structure of $MCR_{ox1-silent}$ shows that the nickel center is axially coordinated by the thiolate sulfur of coenzyme M and the oxygen of the Gln $^{\alpha 147}$ residue.^[5] $MCR_{ox1-silent}$ may be converted to MCR_{ox1} by cryoirradiation (earlier thought of as cryoreduction),^[6] suggesting that both states may share a similar coordination sphere. The MCR_{ox1} state is $S=1/2$ and EPR-active and resembles red1 in that in both cases the unpaired electron appears to reside in a Ni $d_{x^2-y^2}$ orbital. Both the g -value ordering ($g_{||} > g_{\perp} > g_e$) and large hyperfine couplings (25–36 MHz) to the F_{430} nitrogen atoms support this assignment. Thus, a strong case has been that MCR_{ox1} , like red1, also has a Ni^I center.

The oxidation state of MCR_{ox1} has provoked controversy, one that we will not recount here. The latest pulse EPR evidence indicates that the nickel center is most likely Ni^{III} with a $t_{2g}^6 d_{x^2-y^2}^1$ electronic configuration.^[7,8] Though uncommon, such an electronic structure is well-established for synthetic Ni porphyrin^[9] intermediates as well as for the crucial Ni^{III} -methyl/alkyl MCR catalytic intermediates, which have been recently detected by a number of groups.^[10] DFT calculations also supported the viability of such intermediates early on.^[11,12] Interestingly, the recent pulse EPR study^[7] of MCR_{ox1} also indicated that the thiolate sulfur carries a small but non-negligible amount of spin density, about 7% of the total, which cannot be explained in terms of a *pure* $d_{x^2-y^2}^1$ electronic configuration.

If the Ni^{III} -thiolate, or equivalently a high-spin Ni^{II} thiyl radical, description is correct, then MCR_{ox1} joins the growing ranks of bioinorganic intermediates featuring a formally high-valent transition-metal complex with a highly reducing anion as a ligand. High-valent intermediates of the heme-thiolate proteins provide additional examples of such species.^[13] Thus, chloroperoxidase compound II is now recognized as an $S=1$ Fe^{IV} -SCys species.^[14] In the same vein, Groves and co-workers reported a synthetic $S=1$ Fe^{IV} -(OMe)₂ porphyrin species.^[15] Such species are of electronic-structural interest on account of the large number of low-energy states that are potential contenders for the ground state. By and large, heme-based intermediates of this type have been studied in some detail by means of DFT calculations.^[13,14,15b] However, a similar theoretical exploration of MCR_{ox1} has not been reported, a gap in our understanding that we have attempted to address in this study.

Notably, the $d_{x^2-y^2}^1$ configuration of MCR_{ox1} implied by EPR measurements cannot be the only low-energy configuration. Could the unpaired electron not reside in the d_z orbital? Could we not have a low-spin Ni^{II} center bonded to a thiyl radical?^[16] Regular DFT calculations on “high-fidelity” models of the MCR_{ox1} active site cannot shed light on this issue because such calculations can only yield the ground state. Time-dependent DFT calculations are also not expected to be reliable in this context, given their inability to correctly describe long-range charge-transfer transitions.^[17] To explore the electronic-state manifold in more detail, we chose to employ a series of symmetrized models that permitted us to calculate multiple states by fixing different electron occupancies per irreducible representation. Our models are based on a number of monoanionic (monoprotic) porphyrin analogues—oxaporphyrin (OxaP), pyriporphyrin (PyP), and dimethylisoporphyrin (IsoP)—shown in Figure 1. The results of these model studies proved insightful and have helped place the electronic structure of MCR_{ox1} in a much clearer theoretical context.

Methods

The molecules studied were all optimized with the PW91^[18] generalized gradient approximation (GGA) for both exchange and correlation, all-

Table 1. Relative energies [eV] of different spin states of MCR ox1 models. Energy zero levels are indicated in bold.

Configuration	State	Occupations A': α/β A'': α/β	Configuration	PW91	OLYP/PW91	B3LYP/PW91
[Ni(oxaP)(SMe)(AcNH ₂)] ⁺	² A'	A': 77/76 A'': 46/46	(d _{xy}) ² (d _{xz}) ² (d _{yz}) ² (d _{x²-y²}) ¹ , MeS ⁻	0.00	0.00	0.00
	² A''	A': 77/77 A'': 46/45	(d _{xy}) ² (d _{xz}) ² (d _{yz}) ² (d _{x²-y²}) ² , p _y -MeS [•]	0.72	0.59	1.11
[Ni(pyriP)(SMe)(AcNH ₂)] ⁺	² A'	A': 79/78 A'': 47/47	(d _{xy}) ² (d _{xz}) ² (d _{yz}) ² (d _{x²-y²}) ¹ , MeS ⁻	0.00	0.00	0.00
	² A''	A': 79/79 A'': 47/46	(d _{xy}) ² (d _{xz}) ² (d _{yz}) ² (d _{x²-y²}) ² , p _y -MeS [•]	0.72	0.47	1.13
[Ni(isoP)(SMe)(AcNH ₂)] ⁺	² A''	A': 81/81 A'': 50/49	(d _{xy}) ² (d _{xz}) ² (d _{yz}) ² (d _{x²-y²}) ¹ , MeS ⁻	0.00	0.00	0.00
	² A'	A': 82/81 A'': 49/49	(d _{xy}) ² (d _{xz}) ² (d _{yz}) ² (d _{z²}) ¹ , MeS ⁻	0.15	-0.05	0.44
	² A''	A': 82/82 A'': 49/48	(d _{xy}) ² (d _{xz}) ² (d _{yz}) ² (d _{z²}) ² , p _y -MeS [•]	0.60	0.24	0.76

electron Slater-type triple- ζ plus polarization basis sets, and a fine mesh for numerical integration of matrix elements, as implemented in the ADF-2007 program system.^[19] A C_s symmetry constraint was exploited for three model complexes, [Ni(L)(SMe)(AcNH₂)]⁺, in which L = OxaP, PyP, and IsoP and AcNH₂ = acetamide, allowing the optimization of multiple electronic states. In addition, a “high-fidelity”, asymmetric MCR_{ox1} model [Ni(F₄₃₀)(SMe)(AcNH₂)]⁺, with a simplified F₄₃₀ ligand, was also studied.

Although newer pure functionals such as OLYP^[20] and hybrid functionals such as B3LYP^[21] have been shown to perform better than classic pure functionals such as PW91 in a number of applications, the former should not be viewed as perfect. A key flaw of OLYP, B3LYP, etc. is that although they describe stronger metal–ligand bonds quite well, they often greatly exaggerate the lengths of weak metal–ligand bonds *trans* to the aforementioned strong bonds.^[22,23] We were thus concerned that the weak-field AcNH₂ ligand might fall off if we used OLYP, B3LYP, and some of the other functionals that we and others have tended to favor recently. Indeed, this turned out to be a serious problem for high-spin Ni^{II} analogues of the compounds studied here (details not shown), even though a crystal structure of the corresponding biological analogue MCR_{ox1} indicates an O-bound glutamine ligand.^[5]

In light of the above considerations, the discussion below refers almost exclusively to the PW91 optimizations. Having said that, we *did* carry out a limited analysis of the performance of other functionals (OLYP and B3LYP) by means of single-point calculations on the PW91 optimized geometries. Details of the various spin states studied and the energetics obtained with different functionals are shown in Table 1.

Results and Discussion

The oxaporphyrin-based model, [Ni(OxaP)(SMe)(AcNH₂)]⁺: The model complexes in this study were chosen with a view to possible future synthetic modeling. From this point of view, oxaporphyrin,^[24] being one of the more readi-

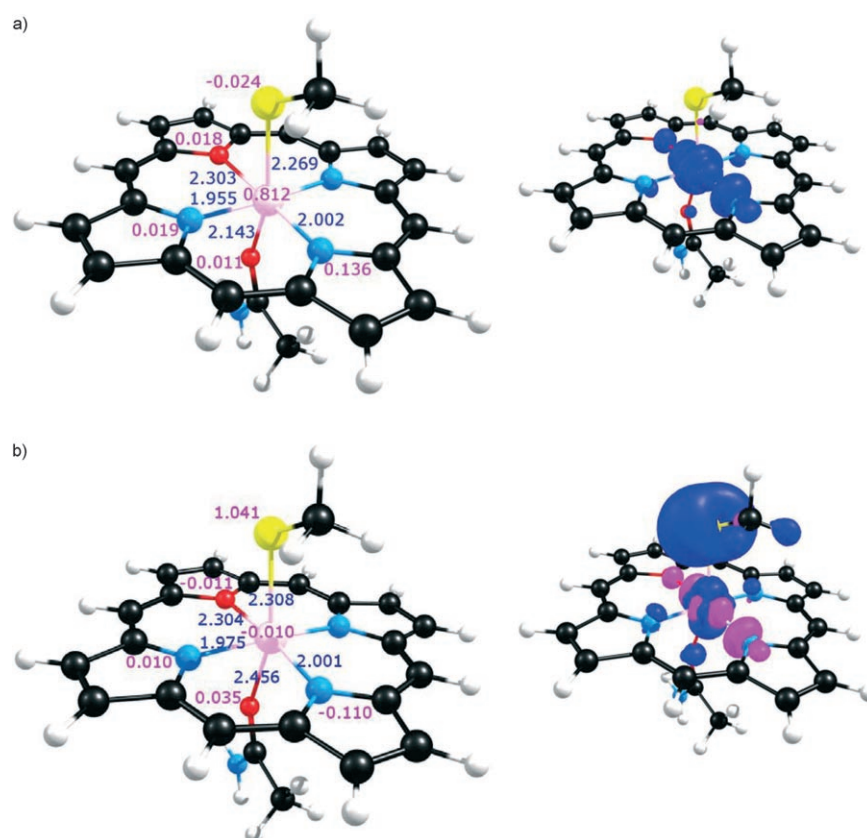


Figure 2. Selected results on the lowest ²A' and ²A'' states of [Ni(OxaP)(SMe)(AcNH₂)]⁺. Bond lengths (Å) and Mulliken spin populations are shown in blue and magenta, respectively. Color code for atoms: C (black), N (cyan), H (ivory), O (red), Ni (pink), and S (yellow). Major and minor spin densities are shown in ultramarine and magenta, respectively.

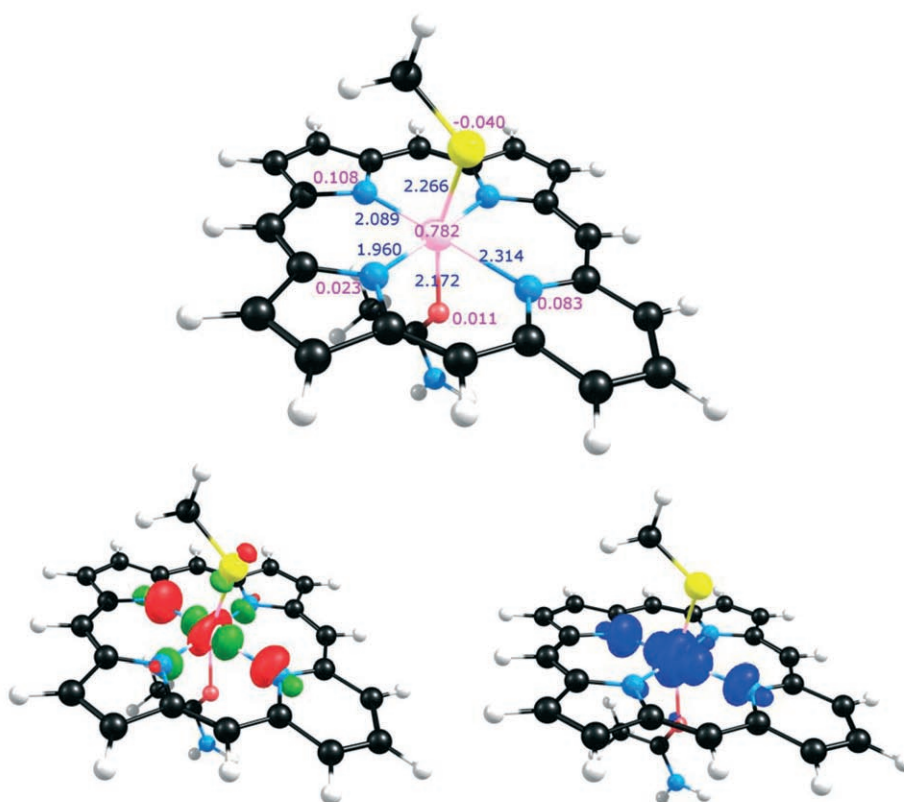
ly accessible monoprotic porphyrin analogues, is an attractive ligand. On the flip side, the oxygen of the oxaporphyrin is a rather weak ligand, somewhat at odds with the N_4 core of F_{430} . Regardless, our ground-state results on $[Ni(OxaP)-(SMe)(AcNH_2)]^+$, summarized in Figure 2, proved illuminating.

Although for brevity and convenience Table 1 describes the electronic configuration as $(d_{xy})^2(d_{xz})^2(d_{yz})^2(d_{x^2-y^2})^1$, the same as that expected for MCR_{ox1} , an examination of the spin-density plot and the SOMO indicates that the quantization of the d-orbital angular momenta is not quite the same as in a fourfold-symmetric metalloporphyrin. The SOMO is

best described as an approximately 1:1 ($d_{x^2-y^2}/d_{z^2}$ hybrid, in effect somewhat of a d_{x^2} orbital, in which the x direction has been identified with the O-Ni-N axis lying on the molecular symmetry plane.

The above detailed comments notwithstanding, the overall ground-state spin-density profile does agree with that qualitatively expected for MCR_{ox1} . As shown in Figure 2, 81% of the majority spin density is localized on the Ni, 14% on the nitrogen *trans* to the oxaporphyrin oxygen, and the remainder is roughly evenly distributed among the other oxaporphyrin nitrogens and the two oxygens. A small minority spin density of -0.024 resides on the thiolate sulfur.

a)



b)

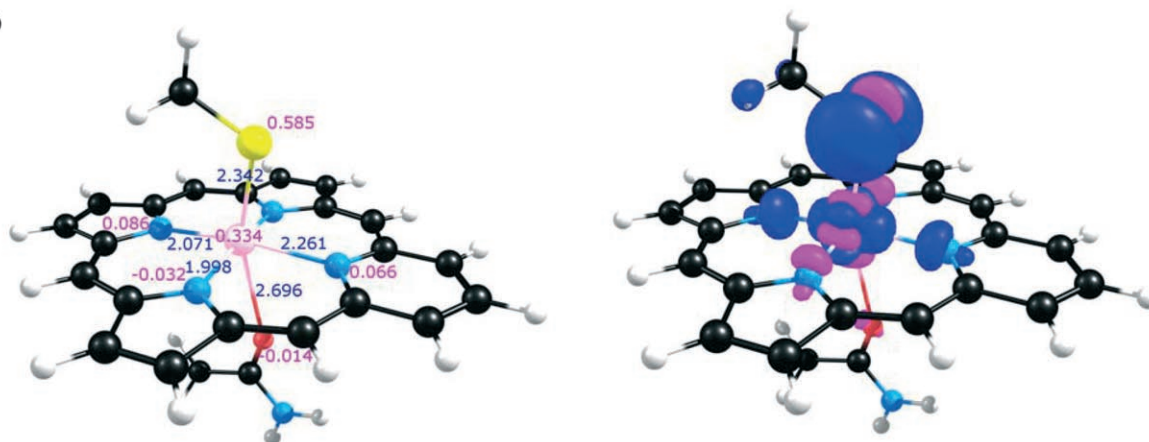


Figure 3. Selected results on the lowest a) $^2A'$ and b) $^2A''$ states $[Ni(PyP)(SMe)(AcNH_2)]^+$. For explanation of text and color code, see Figure 2. Part a) also depicts the SOMO.

Moving a β -spin electron from A'' to fill the β -spin A' hole led to convergence to a $^2A''$ thyl π -radical state, about 0.7 eV (PW91) above the ground state. Some details of this state are shown in part (b) of Figure 2, as well as in Table 1. An examination of the MOs indicates that the nickel center in this state is low-spin Ni^{II} , with a $(d_{xy})^2(d_{xz})^2(d_{yz})^2(d_{x^2-y^2})^2$ configuration, which should be distinguished from the $(d_{xy})^2(d_{xz})^2(d_{yz})^2(d_{z^2})^2$ configuration of "normal" low-spin Ni^{II} porphyrins. Of considerable interest in this connection is the energy of the $(d_{xy})^2(d_{xz})^2(d_{yz})^2(d_{z^2})^1$ state. Unfortunately, regular DFT calculations do not allow us to address this question because both the d_{z^2} and $d_{x^2-y^2}$ orbitals transform as a' for this oxaporphyrin-based model complex.

The pyriporphyrin-based model, $[Ni(PyP)(SMe)(AcNH_2)]^+$: The pyriporphyrin^[25] ligand, a newly reported porphyrin analogue in which a pyrrole unit is replaced by pyridine, provides another excellent symmetric model for the mono-anionic F_{430} ligand. Highlights of our results on $[Ni(PyP)(SMe)(AcNH_2)]^+$, shown in Table 1 and Figure 3, are rather similar to those described above for the oxaporphyrin complex. The Ni spin population in the ground state is slightly smaller than in the oxaporphyrin case, and the equatorial spin populations, on average, are correspondingly slightly higher. That said, the overall spin-density profile once again reflects the shape of a SOMO that is best described as intermediate between $d_{x^2-y^2}$ and d_{x^2} .

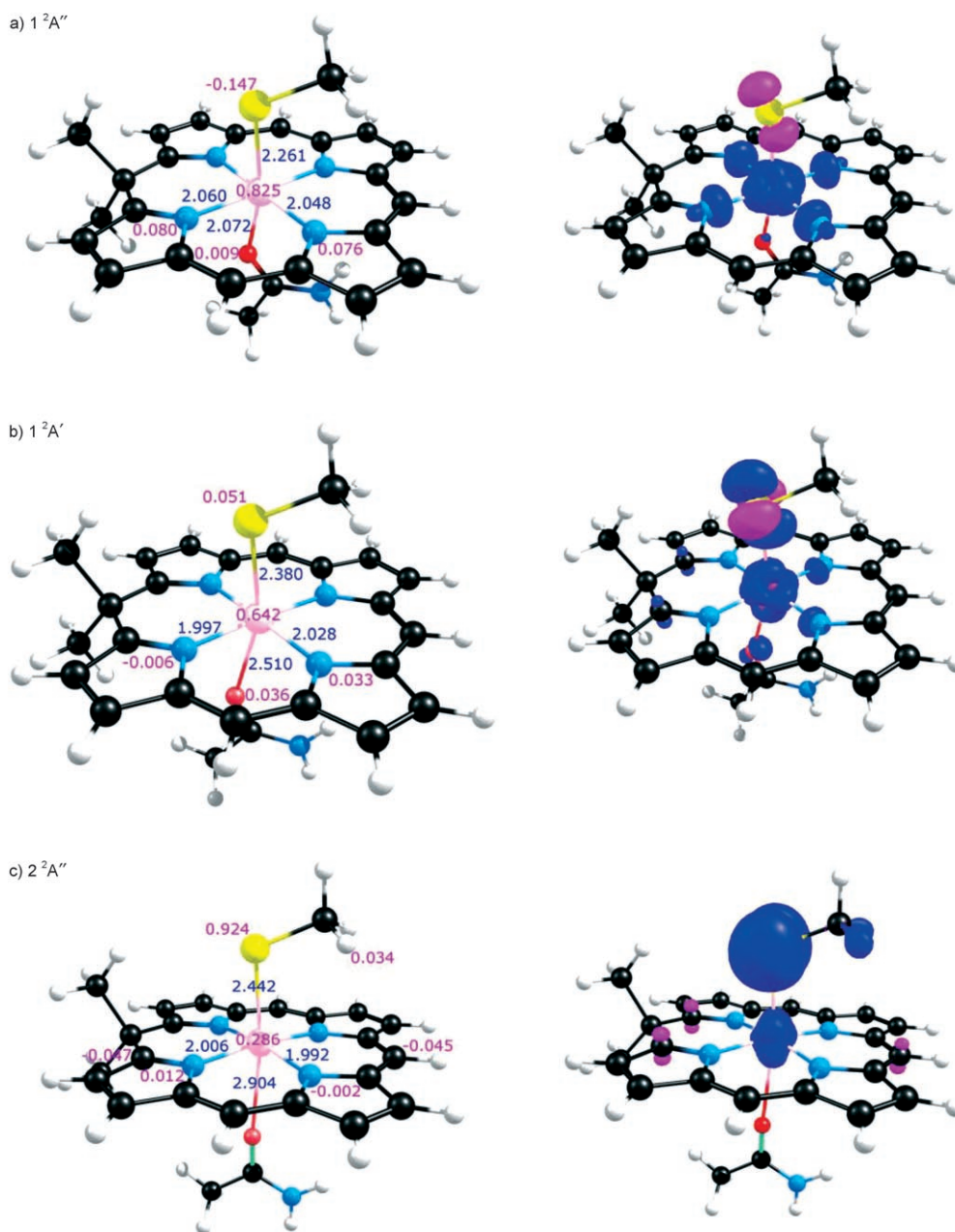


Figure 4. Selected results on three of the lowest states $[Ni(IsoP)(SMe)(AcNH_2)]^+$. For explanation of text and color code, see Figure 2.

The shape of the SOMO merits some comment. Although a *pure* $d_{x^2-y^2}$ orbital is orthogonal to a thiolate σ lone pair, the orthogonality is lifted as d_{z^2} character mixes in. (Stated differently, an Ni d_{xz} orbital is not orthogonal to an S p_z orbital.) Thus, observe (from Figure 3) that the majority-spin HOMO of $[\text{Ni}(\text{PyP})(\text{SMe})(\text{AcNH}_2)]^+$ has a small amplitude on the sulfur atom. Although in this particular case, the sulfur harbors an overall small minority spin population, the exact shape of the SOMO (20.3 % $d_{x^2-y^2}$, 17.4 % d_{z^2}) provides an attractive explanation of how a so-called $(d_{x^2-y^2})^1$ electronic configuration may go hand in hand with a small majority-spin population on the sulfur.

Somewhat coincidentally, the $^2A''$ thiyl π -radical state is once again 0.7 eV (PW91) higher in energy than the ground state. In this case, however, the radical is not as localized on the sulfur as it is in the oxaporphyrin case. The SOMO in this case is best viewed as an a'' $\text{Ni}(d_{yz})\text{-S}(p_y) \pi^*$ MO with roughly 1:2 Ni/S contributions. The significant Ni spin population of 0.334 (see part b, Figure 3) implies that the description of the Ni center as low-spin Ni^{II} with a $(d_{xy})^2(d_{xz})^2(d_{yz})^2(d_{x^2-y^2})^2$ configuration, though valid as a limiting-case description, is less accurate. An Ni^{III} limiting-case description— $(d_{xy})^2(d_{xz})^2(d_{yz})^1(d_{x^2-y^2})^2$ —is also valid to some extent.

The isoporphyrin-based model, $[\text{Ni}(\text{IsoP})(\text{SMe})(\text{AcNH}_2)]^+$: Isoporphyrin, a porphyrin tautomer with interrupted conjugation first postulated by Woodward,^[26] has been known since the 1970s. Our interest in isoporphyrin in relation to this project stems from its symmetry properties. Though nominally of the same point group as our oxaporphyrin- and pyriporphyrin-based models, the mirror plane in the isoporphyrin complex does not pass through the equatorial nitrogens. Accordingly, unlike for the other model complexes, the $d_{x^2-y^2}$ and d_{z^2} orbitals of $[\text{Ni}(\text{IsoP})(\text{SMe})(\text{AcNH}_2)]^+$ are not of the same symmetry, but rather transform as a'' and a' , respectively. This raised the prospect that we should be able to separately optimize for the first time both the $t_{2g}^6 d_{x^2-y^2}^1$ and $t_{2g}^6 d_{z^2}^1$ states of an MCR_{ox1} model, which indeed turned

out to be possible. Thus, three relatively low-energy electronic states (as well as other high-energy states that we will not discuss) could be independently converged for $[\text{Ni}(\text{IsoP})(\text{SMe})(\text{AcNH}_2)]^+$, as shown in Table 1. Highlights of the results are shown in Figure 4.

The $^2A''$ ground state exhibits a clear $(d_{xy})^2(d_{xz})^2(d_{yz})^2(d_{x^2-y^2})^1$ configuration. Unlike in the other cases, the SOMO d contribution is relatively pure $d_{x^2-y^2}$. This is not unexpected because all four isoporphyrin nitrogens share a similar electronic character. However, the Ni spin population, 80 % of the total (as shown in part (a), Figure 4), is essentially the same as in the other cases. The remainder of the majority spin is distributed evenly among the four nitrogens. As in the other cases, a small amount of minority spin (−0.097) resides on the sulfur.

A $^2A'$ $(d_{xy})^2(d_{xz})^2(d_{yz})^2(d_{z^2})^1$ state turned out to be just 0.15 eV (PW91) higher in energy relative to the ground state. The Ni spin population of 64 % of the total is somewhat lower than that in the ground state. Most interestingly, the sulfur in this state exhibits a small but not insignificant majority spin population of 0.051 (see part (b), Figure 4). Given the very low energy of this state, we can easily envision scenarios with less symmetric equatorial ligands in which the d-orbital angular momenta are quantized in such a way as to engender a small majority spin population of 5 % or so on the thiolate sulfur of the ground electronic state. As mentioned above, such a spin population has been observed for MCR_{ox1} .

A second $^2A''$ state proved to be a thiyl π -radical state of the same type as described above for the other complexes. The energy of this state turned out to be 0.6 eV (PW91) relative to the ground state, very much in line with what we found with the other complexes.

Comparative studies of different functionals: To what extent can we trust the above PW91 results? Generally there appears to be little cause for skepticism with respect to the qualitative validity of the results. The PW91 exchange-corre-

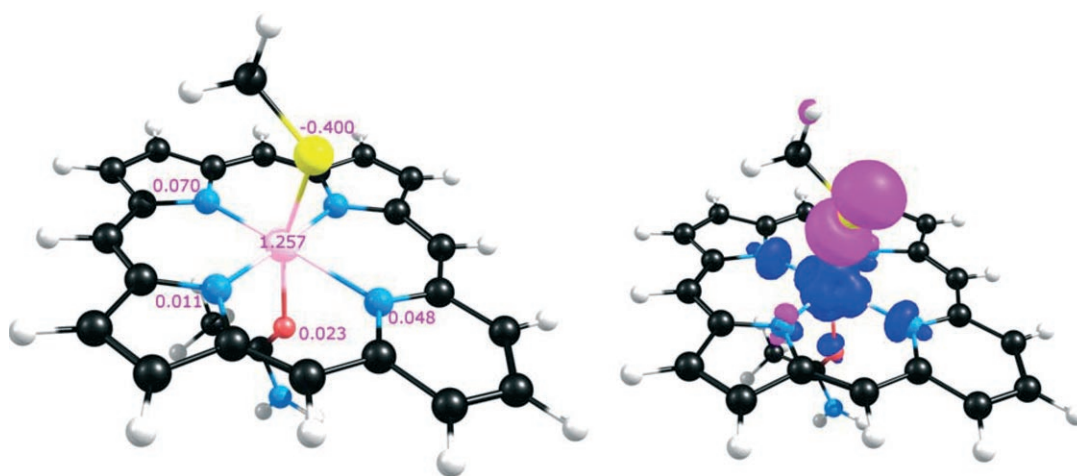


Figure 5. B3LYP spin populations and spin-density plots for the lowest-energy states of $[\text{Ni}(\text{PyP})(\text{SMe})(\text{AcNH}_2)]^+$. For explanation of text and color code, see Figure 2.

lation functional has been widely tested on a variety of transition-metal complexes, notably metalloporphyrins and iron-sulfur clusters. However, like other older pure functionals the PW91 functional sometimes exhibits an undue preference for low-spin states of transition-metal compounds, whereas B3LYP tends to err in the opposite direction.^[22] In this study, however, all pertinent electronic states are doublets. The question of how well DFT (i.e., any of the commonly used functionals) performs with respect to spin-state energetics is, therefore, not expected to be a particularly troublesome one, as far as this study is concerned.

Consistent with these arguments, the relative energies of the different spin states studied are in *qualitative* agreement for the three functionals considered, PW91, OLYP, and B3LYP. B3LYP predicts a somewhat higher energy for the low-spin Ni^{II} thiol radical state than for the other two functionals. Similarly, whereas PW91 and OLYP predict nearly equienergetic $d_{x^2-y^2}^1$ and $d_{z^2}^1$ states for [Ni(IsoP)(SMe)(AcNH₂)]⁺, B3LYP predicts that the latter state is about half an eV higher in energy than the former.

Figure 5 depicts the B3LYP ground-state spin density for [Ni(PyP)(SMe)(AcNH₂)]⁺, chosen as a representative example. Note that the Ni carries significantly more majority spin density (1.257 versus 0.782 with PW91) and, equally, that the sulfur carries a significantly greater amount of minority spin density (−0.400 versus −0.040 with PW91). Careful examination of the blob of spin density on the Ni (shown in ultramarine in Figure 5) shows that it has six distinct bulges, as expected from a superposition of the $d_{x^2-y^2}$ and d_{z^2} orbitals. In other words, B3LYP indicates more of a high-spin Ni^{II} thiol radical-like description for this species, whereas PW91 favors a more covalent Ni^{III} thiolate-like description.^[27] It is important to recognize that the two descriptions are equivalent from an orbital symmetry viewpoint (i.e., with respect to electron occupations per irreducible representation), but differ only with respect to the degree of metal-ligand covalency.

A “high-fidelity” MCR_{ox1} model: The insights obtained above proved invaluable when analyzing the results for a more realistic model of MCR_{ox1}, [Ni(F'₄₃₀)(SMe)(AcNH₂)]⁺. The F'₄₃₀ ligand is the same as that used in our previous modeling

studies of MCR, including one on the then-putative Ni^{III}Me species.^[11b] Selected PW91 results for this complex are shown in Figure 6.

As in our earlier model studies of F₄₃₀,^[11b] the Ni–N distances in the high-fidelity model show a considerable spread, from 1.967 to 2.221 Å, reflecting the electronic asymmetry of the F₄₃₀ (or F'₄₃₀) ligand. At first glance, the spin-density profile of [Ni(F'₄₃₀)(SMe)(AcNH₂)]⁺ is quite similar to those of the ground-state model complexes mentioned above. Closer examination of Figure 6, however, reveals a number of interesting twists:

- 1) The Ni spin population (about 0.7) is somewhat lower than that in the oxaporphyrin- and pyriporphyrin-based models.
- 2) As in the oxaporphyrin- and pyriporphyrin-based model, the spin-density profile reflects a nearly 1:1 $d_{x^2-y^2}/d_{z^2}$ hybrid SOMO. Such a SOMO permits a distinct Ni($d_{x^2-y^2}/d_{z^2}$)–S(p_z) antibonding interaction involving a sulfur σ lone pair.
- 3) Consonant with this orbital interaction, the PW91 spin-density profile of [Ni(F'₄₃₀)(SMe)(AcNH₂)]⁺ exhibits a small but distinct majority spin population of 0.042 on the sulfur.^[28]

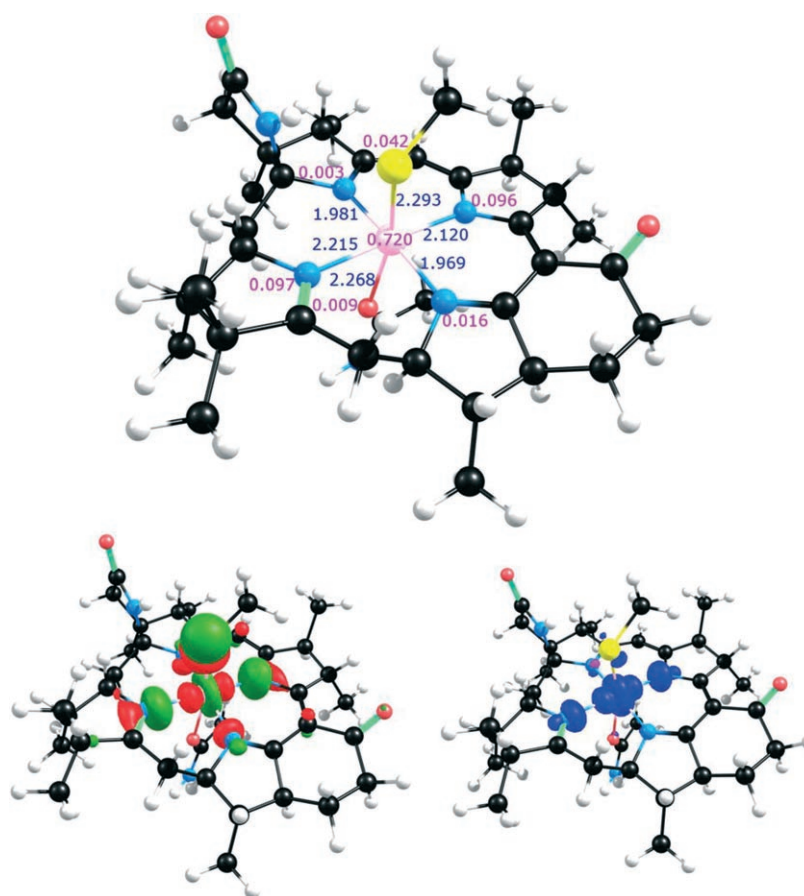


Figure 6. Selected PW91 results on the [Ni(F'₄₃₀)(SMe)(AcNH₂)]⁺. Top: distances and spin populations; bottom left: SOMO; bottom right: spin-density plot. For explanation of text and color code, see Figure 2.

It is tempting to interpret the PW91 sulfur spin population 0.042 as a striking (if qualitative) affirmation of Schweiger and co-workers' conclusions based on their pulse EPR study: "The SOMO is essentially a nickel $d_{x^2-y^2}$ orbital with contributions from the four hydropyrrolic nitrogens and the thiolate sulfur of CoM. The thiolate sulfur has $7 \pm 3\%$ of the spin density."^[7] However, a caveat needs to be added.

A single-point B3LYP calculation on the optimized PW91 geometry of $[\text{Ni}(\text{F}_{430})(\text{SMe})(\text{AcNH}_2)]^+$ reveals a substantially different spin-density profile. With B3LYP, the Ni spin population is 1.311, whereas the sulfur harbors a substantial amount (-0.402) of minority spin. In other words, the situation is entirely analogous to that depicted for $[\text{Ni}(\text{PyP})(\text{SMe})(\text{AcNH}_2)]^+$ in Figure 5. In this case, however, Schweiger and co-workers' pulse EPR study permits us to arrive at a conclusion with regard to the relative merits of the B3LYP and PW91 spin densities. The experimental results clearly rule out a large spin population on the sulfur, such as that predicted by B3LYP. Thus, under the circumstances, it is tempting to view the PW91 spin density as representative of reality.

Conclusion

When it comes to delineating complicated enzymatic reaction mechanisms, computer simulations may readily go astray in the absence of adequate guidance from experiment. However, for a given enzymatic intermediate, DFT calculations are generally eminently suitable for judging whether a proposed electronic-structural description makes chemical sense or not. As far as MCR_{ox1} is concerned, the present calculations indicate that a Ni^{III} -thiolate, or equivalently a high-spin Ni^{II} thyl radical, description is a reasonable one. Essentially the same ground-state description was obtained for three symmetrized models as well as for a more realistic structure.

Although the spin density of the various model complexes is broadly interpretable as arising from an unpaired electron in a nickel $d_{x^2-y^2}$ orbital, careful examination of the SOMO indicates that this orbital may also have a substantial amount of d_{z^2} character. (In other words, the spin density in the equatorial plane is not quite fourfold symmetric.) The d_{z^2} contribution to the SOMO permits an $\text{Ni}(d_{x^2-y^2}/d_{z^2})\text{-S}(p_z)$ antibonding interaction involving a thiolate σ lone pair, which would otherwise be symmetry-forbidden. With pure functionals such as PW91, this orbital interaction manifests itself in a small but distinct majority spin population of 0.042 on the sulfur in our most realistic MCR_{ox1} model, which is in reasonable agreement with that (about 7%) derived from a pulse EPR study.^[7]

Acknowledgement

This work was supported by the Research Council of Norway. We thank Profs. J. Telser and B.M. Hoffman for helpful advice.

- [1] S. Shima, R. K. Thauer, *Curr. Opin. Microbiol.* **2005**, *8*, 643–648.
- [2] a) T. DiMarco, A. Bobik, R. S. Wolfe, *Annu. Rev. Biochem.* **1990**, *59*, 355–394; b) R. S. Wolfe, *Annu. Rev. Microbiol.* **1991**, *45*, 1–35.
- [3] R. K. Thauer, *Microbiology* **1998**, *144*, 2377–2406.
- [4] a) S. W. Ragsdale in *The Porphyrin Handbook* (Eds.: K. M. Kadish, K. M. Smith, R. Guilard), Elsevier, San Diego, CA, **2003**, Vol. 11, pp. 205–228; b) A. Ghosh, T. Wondimagegn, H. Ryeng, *Curr. Opin. Chem. Biol.* **2001**, *5*, 744–750; c) J. Telser, *Struct. Bonding (Berlin)* **1998**, *91*, 31–63.
- [5] U. Ermler, W. Grabase, S. Shima, M. Goubeaud, R. K. Thauer, *Science* **1997**, *278*, 1457–1462.
- [6] J. Telser, R. Davydov, Y.-C. Horng, S. W. Ragsdale, B. M. Hoffman, *J. Am. Chem. Soc.* **2001**, *123*, 5853–5860.
- [7] J. Harmer, C. Finazzo, R. Piskorski, C. Bauer, B. Jaun, E. C. Duin, M. Goenrich, R. K. Thauer, S. Van Doorslaer, A. Schweiger, *J. Am. Chem. Soc.* **2005**, *127*, 17744–17755.
- [8] For additional ENDOR studies of MCR derivatives, see: a) C. Finazzo, J. Harmer, C. Bauer, B. Jaun, E. C. Duin, F. Mahrert, M. Goenrich, R. K. Thauer, S. van Doorslaer, A. Schweiger, *J. Am. Chem. Soc.* **2003**, *125*, 4988–4989; b) J. Telser, Y.-C. Horng, D. F. Becker, B. M. Hoffman, S. W. Ragsdale, *J. Am. Chem. Soc.* **2000**, *122*, 182–183.
- [9] a) J. Seth, V. Palaniappan, D. F. Bocian, *Inorg. Chem.* **1995**, *34*, 2201–2206; b) M. W. Renner, K. M. Barkigia, D. Melamed, J. P. Gisselbrecht, N. Y. Nelson, K. M. Smith, J. Fajer, *Res. Chem. Intermed.* **2002**, *28*, 741–759.
- [10] a) D. Hinderberger, R. R. Piskorski, M. Goenrich, R. K. Thauer, A. Schweiger, J. Harmer, B. Jaun, *Angew. Chem.* **2006**, *118*, 3684–3689; *Angew. Chem. Int. Ed.* **2006**, *45*, 3602–3607; b) N. Yang, M. Reiher, M. Wang, J. Harmer, E. C. Duin, *J. Am. Chem. Soc.* **2007**, *129*, 11028–11029; c) M. Dey, J. Telser, R. C. Kunz, N. S. Lees, S. W. Ragsdale, B. M. Hoffman, *J. Am. Chem. Soc.* **2007**, *129*, 11030–11032.
- [11] a) A. Ghosh, T. Wondimagegn, E. Gonzalez, I. Halvorsen, *J. Inorg. Biochem.* **2000**, *78*, 79–82; b) T. Wondimagegn, A. Ghosh, *J. Am. Chem. Soc.* **2001**, *123*, 5680–5683; For a recent follow-up study, see: c) J. Conradie, T. Wondimagegn, A. Ghosh, *J. Phys. Chem. B* **2008**, *112*, 1053–1056.
- [12] For DFT studies of MCR_{red1} ($\text{Ni}^{\text{I}}\text{F}_{430}$), see: a) T. Wondimagegn, A. Ghosh, *J. Am. Chem. Soc.* **2000**, *122*, 6375–6381; b) K. P. Jensen, U. Ryde, *J. Porphyr. Phthalocya.* **2005**, *8*, 581–606.
- [13] R. K. Behan, M. T. Green, *J. Inorg. Biochem.* **2006**, *100*, 448–459.
- [14] K. L. Stone, R. K. Behan, M. T. Green, *Proc. Natl. Acad. Sci. USA* **2006**, *103*, 12307–12310.
- [15] a) J. T. Groves, R. Quinn, T. J. McMurphy, M. Nakamura, G. Lang, B. Boso, *J. Am. Chem. Soc.* **1985**, *107*, 354–360; b) J. Conradie, I. H. Wasbotten, A. Ghosh, *J. Inorg. Biochem.* **2006**, *100*, 502–506.
- [16] Such a formulation has been proposed by: J. L. Craft, Y.-C. Horng, S. W. Ragsdale, T. C. Brunold, *J. Am. Chem. Soc.* **2004**, *126*, 4068–4069.
- [17] For a discussion, see: H. Nakano, T. Nakajima, T. Tsuneda, K. Hirao in *Theory and Applications of Computational Chemistry: The First Forty Years* (Eds.: C. E. Dykstra, G. Frenking, K. S. Kim, G. E. Scuseria), Elsevier, Amsterdam, **2005**, pp. 507–557.
- [18] J. P. Perdew, J. A. Chevary, S. H. Vosko, K. A. Jackson, M. R. Pederson, D. J. Singh, C. Fiolhais, *Phys. Rev. B* **1992**, *46*, 6671–6687; Erratum: J. P. Perdew, J. A. Chevary, S. H. Vosko, K. A. Jackson, M. R. Pederson, D. J. Singh, C. Fiolhais, *Phys. Rev. B* **1993**, *48*, 4978.
- [19] The ADF program system was obtained from Scientific Computing and Modeling, Amsterdam (<http://www.scm.com/>). For a description of the methods used in ADF, see: G. T. Velde, F. M. Bickelhaupt, E. J. Baerends, C. F. Guerra, S. J. A. Van Gisbergen, J. G. Snijders, T. Ziegler, *J. Comput. Chem.* **2001**, *22*, 931–967.

- [20] The OLYP functional is based on the OPTX exchange functional (N. C. Handy, A. J. Cohen, *J. Mol. Phys.* **2001**, *99*, 403–412) and the LYP correlation functional (C. Lee, W. Yang, R. G. Parr, *Phys. Rev. B* **1988**, *37*, 785–789).
- [21] a) J. Stephens, F. J. Devlin, C. F. Chabalowski, M. J. Frisch, *J. Phys. Chem.* **1994**, *98*, 11 623–11 627; b) M. A. Watson, N. C. Handy, A. J. Cohen, *J. Chem. Phys.* **2003**, *119*, 6475–6481; c) R. H. Hertwig, W. Koch, *Chem. Phys. Lett.* **1997**, *268*, 345–351.
- [22] A. Ghosh, *J. Biol. Inorg. Chem.* **2006**, *11*, 712–724.
- [23] F. Neese, *J. Biol. Inorg. Chem.* **2006**, *11*, 702–711.
- [24] For a convenient synthetic route to oxaporphyrins, see: A. Srinivasan, B. Sridevi, M. V. R. Reddy, S. J. Narayanan, T. K. Chandrashekar, *Tetrahedron Lett.* **1997**, *38*, 4149–4152.
- [25] R. Mysliborski, L. Latos-Grazynski, L. Szterenberg, *Eur. J. Org. Chem.* **2006**, 3064–3068.
- [26] R. B. Woodward, *Ind. Chim. Belge* **1962**, *27*, 1293.
- [27] For a similar difference between PW91 and B3LYP spin-density profiles for NO complexes, see: J. Conradie, A. Ghosh, *J. Phys. Chem. B* **2007**, *111*, 12 621–12 624.
- [28] DFT modeling studies of heme-thiolate proteins have shown that the thiolate spin density may be modulated by environmental factors such as a hydrogen-bond donor; for example, see F. Ogliaro, S. Cohen, S. P. de Visser, S. Shaik, *J. Am. Chem. Soc.* **2000**, *122*, 12 892–12 893.

Received: April 4, 2008

Revised: July 2, 2008

Published online: September 24, 2008